JOURNAL OF SOLID STATE CHEMISTRY 19, 331–351 (1976)

Solid State Reactions in the System $Nb_2O_5.WO_3$: An Electron Microscopic Study

H. OBAYASHI* AND J. S. ANDERSON†

Inorganic Chemistry Laboratory, University of Oxford, Oxford, England

Received July 26, 1976

Lattice imaging electron microscopy has been used to study the mechanism of solid state reactions of the type: $A_s \rightarrow B_s + C_s$, in which the product B is able to intergrow coherently with the starting material A, but the product C cannot do so. C must be formed by a fully reconstructive, heterogeneous process; formation of B is only partially reconstructive, and essentially homogeneous. Reactions were the reversible phase reactions in the system Nb_2O_5–WO_3: disproportionation of the $(5 \times 4)_1$ block structures of $8Nb_2O_5.5WO_3$, to form $(4 \times 4)_1$ blocks of $7Nb_2O_5.3WO_3$ as coherent product, and that of $9Nb_2O_5.8WO_3$ (with $(5 \times 5)_1$ blocks), forming $(5 \times 4)_1$ blocks of $8Nb_2O_5.5WO_3$ as coherent product. The coherent product structure is formed in isolated rows of blocks, or small packets of such rows, running across each crystal. The reaction does not work in progressively from some surface initiating step, with an interface between unchanged and converted material, but represents a block-by-block conversion, linearly propagated. Nb_2O_5 and WO_3 must be abstracted, in appropriate stoichiometric ratio, from each block but must ultimately reach and react at the surface, to form the incoherent product (a pentagonal tunnel network structure, in both cases). Some homogeneous transport process involving lattice diffusion must be invoked. Domains of highly anomalous structure, regarded as relicts of transient conditions, are occasionally observed. From reactions at relatively low temperatures, these have structures that can be regarded as partially ordered nonstoichiometric solid solutions; after prolonged heating, and at higher temperatures they form well ordered strips of metastable block structures. Both types represent strong, spontaneous fluctuations of composition, which impose a corresponding structure locally. These fluctuations may be associated with the transport of WO_3 and Nb_2O_5 away from the locus of reaction. Evidence about the mechanism of the reactions, the role of dislocations and the nature of cooperative processes is considered.

Except for reactions of the simplest type, it is rarely possible to identify the mechanism of solid state reactions explicitly, in the terms of the displacements and the diffusion rates of the component atoms. In the more complex structures, at least, the processes are likely to follow some structurally determined path, which can be inferred only indirectly, and even a qualitative elucidation of such topochemical mechanisms, would be useful. As part of our development of lattice imaging methods of electron microscopy, we have examined several reaction systems, with the idea that the ability to detect and interpret local perturbations of structure might make it possible to deduce some of the steps whereby one crystal structure is converted into another. Accessible to study in this way are "homogeneous" reaction processes—that is, partially reconstructive processes or precursor stages in phase transformations—in which coherence between the initial structure and the reaction product (or reaction intermediate) is conserved. This possibility was exploited in an investigation of the oxidation of $Nb_{12}O_{29}$,

* Permanent address: Central Research Laboratory, Hitachi Ltd., Kokubunji, Tokyo 185, Japan.

† Present address: Edward Davies Chemical Laboratories, University College of Wales, Aberystwyth, Dyfed, SY23 1NE, U.K.

a partially reconstructive reaction (*1*). In this paper we consider some phase reactions of the general type

$$A(\text{solid}) \rightarrow B(\text{solid}) + C(\text{solid})$$

in which one of the product phases (B) can retain coherence with the starting material A. In so far as one product phase C, is incoherent, the over-all course of such reactions necessarily follows the classical pattern of nucleation and growth; what can be examined, however, is both the topochemical relation between reactant A and product B, and any residual evidence for precursor stages, within the reactant structure, that generate the supersaturation needed to nucleate the incoherent product C.

The requisite for such a study is a system that lends itself to effective lattice imaging and that involves one or more solid state reactions in a convenient temperature range. We have therefore examined phase reactions in the system Nb_2O_5–WO_3, the equilibria in which have been thoroughly studied by Roth and Waring (*2*). Their equilibrium diagram (Fig. 1) shows a succession of intermediate phases, some of which are stable only within a restricted range of temperature. They lend themselves to lattice imaging and the phase reactions are reversible.

All these phases have structures derived from the DO_9 (ReO_3) type, with networks of octahedral [MO_6] groups linked by sharing the oxygen atoms at their vertices. The end member, WO_3, has the DO_9 structure in distorted form. Along the series, as the ratio $O:(W+Nb)$ changes from 3.0 to 2.5, the stoichiometry is accommodated by a succession of well-established topological transformations. For compositions MO_x, with $3.0 \geqslant x >$ ca 2.80, the DO_9 structure is collapsed by crystallographic shear. For ca $2.80 > x \geqslant 2.67$, an apparently different type of structure supervenes, but it is also derived from the DO_9 type through the operation of what Hyde and O'Keeffe (*3*) have termed rotary shear. This creates pentagonal tunnels in a network of vertex-sharing octahedra with the net formula MO_3; the stoichiometric ratio MO_x is attained by filling some of these tunnels with strings of atoms ···–O–Nb–O–Nb–

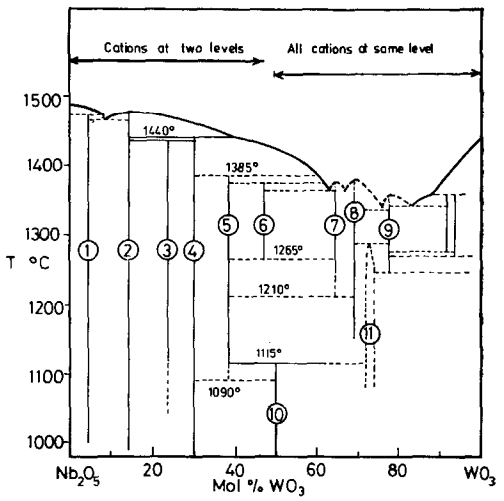

FIG. 1. Equilibrium diagram for system Nb_2O_5–WO_3. Intermediate phases: (A) Block structures: (1) $13Nb_2O_5.WO_3$; (2) $6Nb_2O_5.WO_3$; (3) $13Nb_2O_5.4WO_3$; (4) $7Nb_2O_5.3WO_3$; (5) $8Nb_2O_5.5WO_3$; (6) $9Nb_2O_5.8WO_3$. (B) Pentagonal tunnel structures: (7) $6Nb_2O_5.11WO_3$; (8) $4Nb_2O_5.9WO_3$; (9) $2Nb_2O_5.7WO_3$; (10) $Nb_2O_5.WO_3$; (11) "$3Nb_2O_5.8WO_3$".

O–··· so that the tunnel cations are 7-coordinate. This is the basis of the tetragonal tungsten bronze structures, exemplified by the congruently melting $4Nb_2O_5.9WO_3$, or $(NbO)_4Nb_{12}W_{18}O_{90}$, in which 4 out of 12 pentagonal tunnels are filled, with a (3×1) superlattice of the simple tetragonal tungsten bronze (TTB) type. For $2.67 > x \geqslant 2.50$, the polyhedron network reverts to an orthogonal array, collapsed by the operation of two sets of crystallographic shear planes (*CS* planes) and generating a succession of block structures between $9Nb_2O_5.8WO_3$ ($W_8Nb_{18}O_{69}$, with $(5 \times 5)_1$ blocks) and H–Nb_2O_5.

A further point concerning the topology of these structures is important. In all the structures included within the composition range $3.0 \geqslant x > 2.67$, the cations are coplanar. In principle, changes in composition could be continuously accommodated by coherent intergrowth of isolated elements or extended domains of differing structure and composition. That a succession of discrete phases has been observed is due to the thermodynamics of ordering, rather than to structural constraints, and these intermediate phases may

well tolerate some variability of gross composition. This is the case for the tetragonal tungsten bronze networks (*4*); no systematic study has as yet been carried out on the transition between *CS* phases and pentagonal tunnel structures at about $x = 2.8$. In the composition range $2.67 > x \geqslant 2.50$, however, it is inherent in the block structures that cations should be located at two levels, $y = 0$ and $y = \frac{1}{2}$, separated by one half the octahedron diagonal length. Pairs of adjacent block structures can intergrow freely in perfect coherence, but no coherent composition plane can be found to permit intergrowth between block structures and pentagonal tunnel structures. There is a discontinuity in the topological transformation, which is important mechanistically and kinetically in any phase reaction that generates or involves structures of the two different kinds.

Table I, based on the equilibrium diagram, summarizes the reactions within the composition range 30–70 mol% WO_3, written as disproportionations of a single phase above its upper, or below its lower, stability limit. Disproportionations can be followed more readily than recombination reactions, since a single reactant can be prepared, quenched from a high temperature and fully characterized before and after reaction. The structure and status of "$6Nb_2O_5.11WO_3$" are not yet clear; Roth and Waring state that it probably melts congruently, but we did not obtain uniform products in our systematic electron microscope study. Reactions 6 and 7 have therefore not been studied. Reaction 8 is unique, as being the only disproportionation in which block structures are generated (as the incoherent phase) from pentagonal tunnel structures. We shall discuss this and other processes within the tunnel structures in a later paper; here we restrict consideration to the changes taking place during reaction within the block structures, as starting materials.

It will be clear from Table I that, in reactions 1, 2, 3, and 4, the product block structures should be capable of coherent intergrowth with the parent phase, but this would not be the case in reaction 5 unless the 8 : 5 compound were formed and retained as an intermediate product. In each of these reactions, it should be possible, by high resolution microscopy carried out on incompletely reacted materials,

TABLE I

PHASE REACTIONS IN THE SYSTEM Nb_2O_5–WO_3 (30–70 mol% WO_3)

A	1	$8Nb_2O_5.5WO_3 \rightarrow 7Nb_2O_5.3WO_3 + Nb_2O_5.WO_3$ $(5 \times 4)_1$ blocks $\quad (4 \times 4)_1$ blocks $\quad$ pentag. tunnels	$T < 1090°C$
B	2	$9Nb_2O_5.8WO_3 \rightarrow 8Nb_2O_5.5WO_3 +$ "$6Nb_2O_5.11WO_3$" $(5 \times 5)_1$ blocks $\quad (5 \times 4)_1$ blocks $\quad$ TTB	$1210° < T < 1265°C$
	3	$9Nb_2O_5.8WO_3 \rightarrow 8Nb_2O_5.5WO_3 + 4Nb_2O_5.9WO_3$ $(5 \times 5)_1$ blocks $\quad (5 \times 4)_1$ blocks $\quad$ TTB	$1115° < T < 1210°C$
	4	$9Nb_2O_5.8WO_3 \rightarrow 8Nb_2O_5.5WO_3 + Nb_2O_5.WO_3$ $(5 \times 5)_1$ blocks $\quad (5 \times 4)_1$ blocks $\quad$ pentag. tunnels	$1090° < T < 1115°C$
	5	$9Nb_2O_5.8WO_3 \rightarrow 7Nb_2O_5.3WO_3 + Nb_2O_5.WO_3$ $(5 \times 5)_1$ blocks $\quad (4 \times 4)_1$ blocks $\quad$ pentag. tunnels	$T < 1090°C$
C	6	"$6Nb_2O_5.11WO_3$" $\rightarrow 8Nb_2O_5.5WO_3 + 4Nb_2O_5.9WO_3$ TTB $\quad (5 \times 4)_1$ blocks $\quad$ TTB	$1115° < T < 1210°C$
	7	"$6Nb_2O_5.11WO_3$" $\rightarrow Nb_2O_5.WO_3 + 4Nb_2O_5.9WO_3$ TTB $\quad$ pentag. tunnels $\quad$ TTB	$T < 1115°C$
D	8	$Nb_2O_5.WO_3 \rightarrow 8Nb_2O_5.5WO_3 + 4Nb_2O_5.9WO_3$ pentag. tunnels $\quad (5 \times 4)_1$ blocks $\quad$ TTB	$1115° < T < 1265°C$

to determine the morphology, distribution and microstructure of the reaction product: whether formed topotactically on the surface of the parent as discrete crystals, or formed as coherent and extensive domains by growth from some nucleus, or produced in discrete units by a succession of isolated reaction events. All the reactions involve a nett loss of WO_3 from the initial material and it appears to us probable, although not proven, that the topologically incompatible pentagonal tunnel structures are formed via a gas-phase transfer of WO_3, which reacts at the surface of other reactant crystals by nucleation, reconstruction and growth. Some heterogeneous transfer of WO_3 is necessary and if—as proves to be the case—this reaction step is kinetically hindered (e.g., if some excess chemical potential of WO_3 is needed to attain a significant rate of nucleation and growth of the incoherent product), metastable structures might well be created as transitional products. Precursor steps of this kind might be identifiable by electron microscopy, as faulted regions of structure. Since internal transfer processes (lattice diffusion) and surface transfer processes (surface diffusion and vaporization) will both be greatly accelerated at high temperatures, the clearest evidence for any precursor steps is likely to come from reactions carried out at the lowest possible temperatures. Reaction 1, carried out at 900°C, is

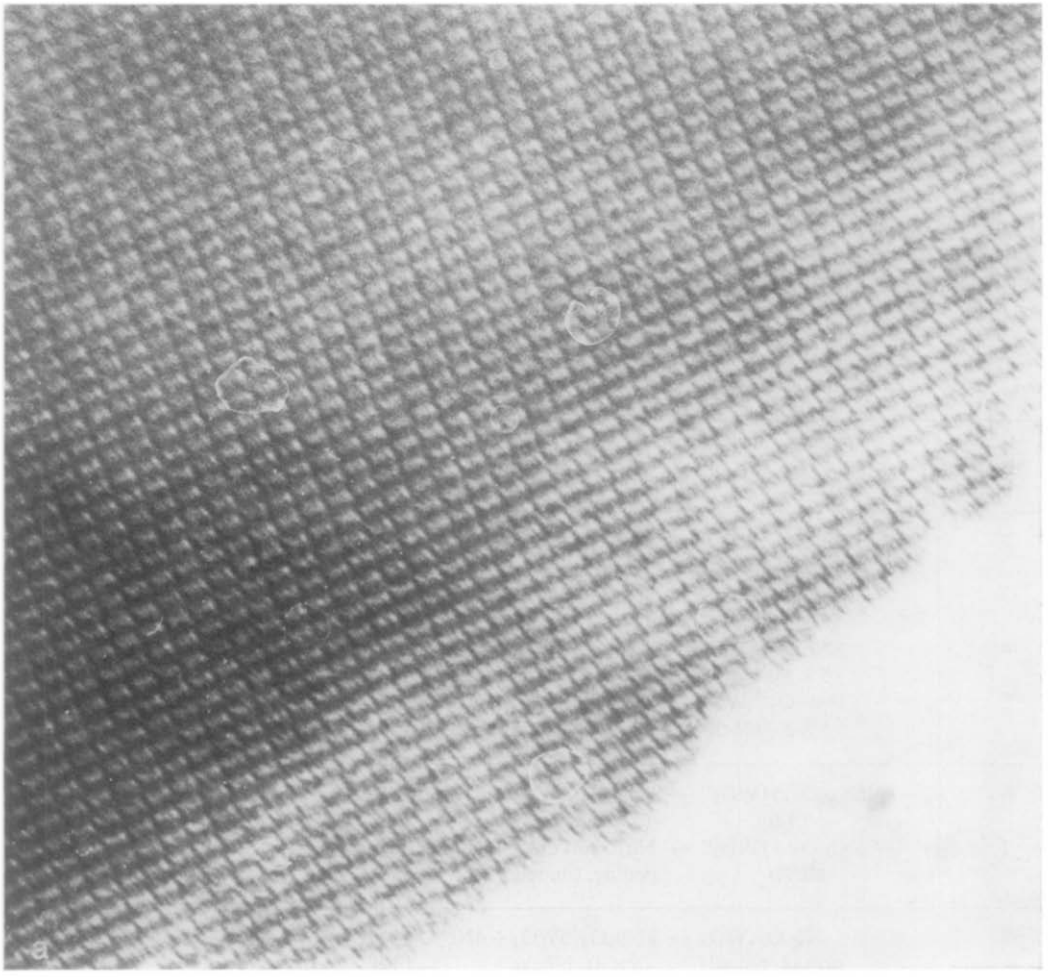

FIG. 2. Well-ordered structures of starting materials. (a) $(5 \times 4)_i$ structure of $8Nb_2O_5.5WO_3$.

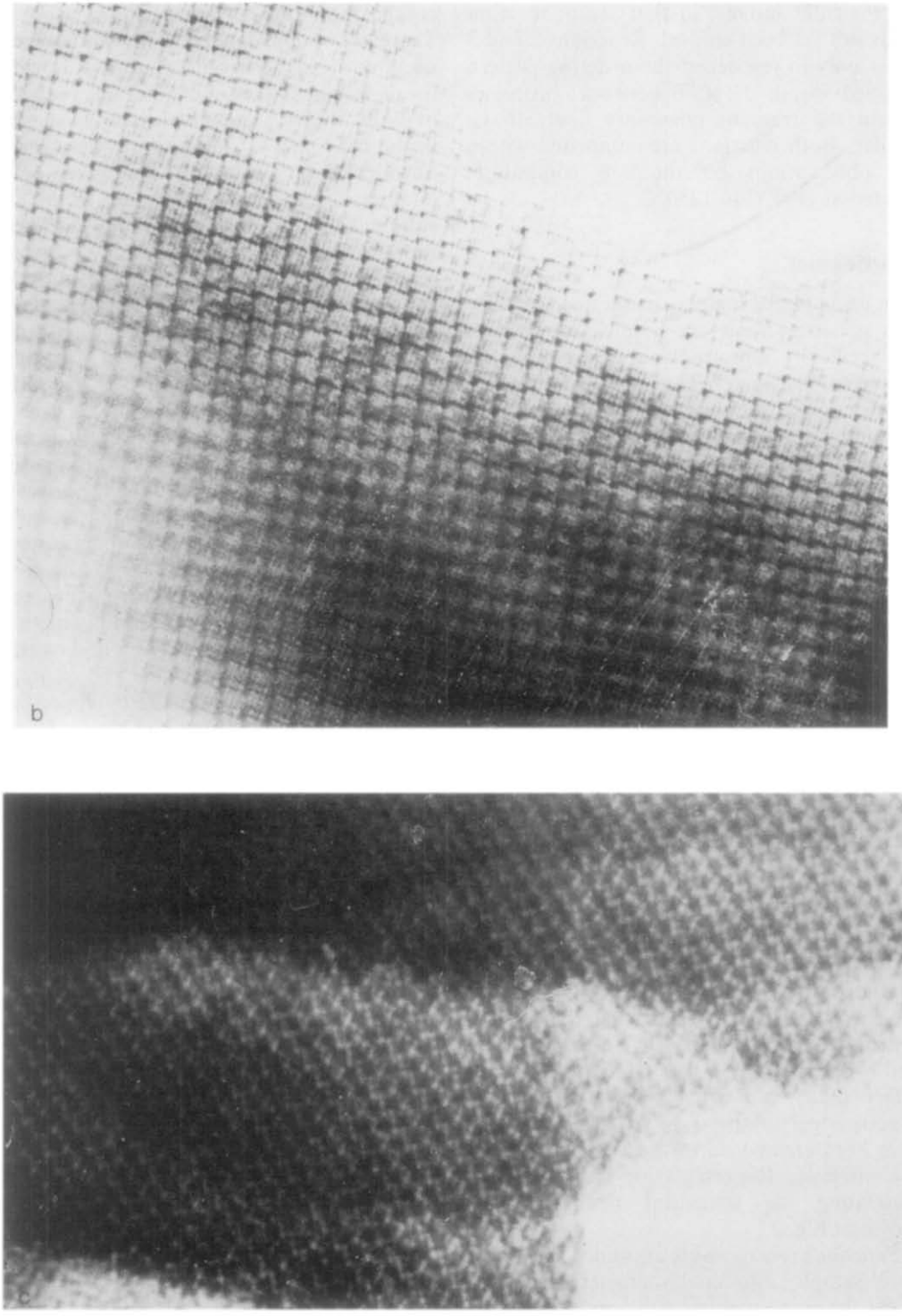

FIG. 2. (b) $(5 \times 5)_1$ structure of $9Nb_2O_5 \cdot 8WO_3$. (c) Pentagonal tunnel structure of $Nb_2O_5 \cdot WO_3$.

of particular interest in that sense; reaction 5 has not yet been studied. Reactions 2 and 3 differ only in respect of the ordering pattern attained within the TTB network; processes within the reactant phase are likely to be similar. Both reactions are comprised within the observations on the 9:8 compound, reacted at 1145°C to 1250°C.

Experimental

In using lattice imaging methods to identify how a perfect structure becomes perturbed, it is critically important to ensure that the perturbations observed are the genuine consequences of reaction, and not intrinsic faults. Starting materials must therefore be characterized with great care. $7Nb_2O_5.3WO_3$, $8Nb_2O_5.5WO_3$, $9Nb_2O_5.8WO_3$ and $Nb_2O_5.WO_3$ were prepared from Johnson Matthey Specpure oxides by the methods described previously (*4*); the three block structure phases were finally annealed at 1300°C in sealed platinum capsules for 70–80 hours, then quenched to room temperature.

The identity and monophasic character of each preparation was checked by X-ray diffraction, using a Hägg–Guinier camera; diffraction patterns were compared with the published data of Roth and Wadsley (*5*) and Roth and Waring (*2*). To characterize their microstructure, samples of each were examined by lattice imaging and micrographs were recorded from a sufficient number of crystal fragments of each sample to be regarded as representative. In our experience such a search procedure is inherently biased in favor of the detection of faults that may be present in low abundance. After the 1300°C anneal, all the samples were exceedingly well ordered, with so few faults or extended defects that we are confident that the types of structural perturbation discussed below must have been created during reaction, and were not intrinsic. Representative lattice images illustrating the structural perfection are shown in Fig. 2.

Reaction processes were examined by sealing small samples into small-diameter silica capsules; the empty volume was kept as small as possible in order to minimize any change of composition due to vaporization of WO_3. There was some tendency for reduction to occur at the higher temperatures, as shown by the darkening of the solid. Since any reduction of W(*vi*) to W(*v*) is equivalent to an increase in the $Nb_2O_5:WO_3$ ratio, it was desirable to obviate it as far as possible. To this end, in the later experiments, the void space in the capsules was filled with oxygen to 150–400 Torr at room temperature before sealing, so that the oxygen pressure was maintained well above the dissociation pressure. The sealed capsules were introduced into the furnace, preheated to the reaction temperature, and were withdrawn after periods of from 1 hour to 500 hours, then quenched in ice water.

The kinetics of these disproportionation reactions are quite unknown and, in the light of the results set out below, would be difficult to formulate. For the present purposes, the requirement was to catch the process at such incomplete, intermediate stages of transformation as would yield useful structural evidence.

Lattice imaging was carried out by methods that are now standard. Finely ground material was dispersed on carbon films and examined with a Siemens Elmiskop 102 equipped with a tilting, *z*-translation stage. Thin (< 10 nm) fracture edges or flakes were sought, oriented with the short (0.4 nm) crystallographic axis parallel to the electron beam, and micrographs taken in a through-focal series bracketing the optimum defocus, using all diffracted beams transmitted by a 40 μm objective aperture. The resulting lattice images approximate to the projected charge density distribution in the crystals; local structure is revealed directly, and local composition can be inferred from the topology of the block structures, or from the extent of tunnel occupancy in the TTB structures. In this particular work, significant features occasionally extended into, or were formed in, the thicker regions of crystal, for which the projected charge density approximation is invalid. It was nevertheless practicable, in many cases, to discern the dimensions and connectivity of the ReO_3-like blocks and thus to map the structure. Not infrequently we observed the recovery of phase coherence in thick crystal (>100 nm thick), as reported by Fejes, Iijima, and Cowley (*6*),

restoring the detailed information content of the lattice images.

Results

As is discussed later, the disproportionation of $8Nb_2O_5.5WO_3$ and that of $9Nb_2O_5.8WO_3$ are closely analogous, both in formal description and in mechanism. It is convenient first to set out the general characteristics of the incompletely reacted materials and then to consider the mechanistic implications of the results. Our attention was concentrated primarily on the homogeneous aspect of reaction processes within the block structure oxides, and less interest was attached to the perfection of ordering and attainment of equilibrium composition in the pentagonal tunnel structure products that were formed incoherently by a heterogeneous route.

Disproportionation of $8Nb_2O_5.5WO_3$

This process, occurring at temperatures below its lower stability limit (1090°C) is of particular interest as the low reaction temperature should give a chance to discriminate between alternative (or sequential) processes of differing activation energy. The broad results observed at 900°C are summarized in Table II.

After 23 hours, the crystals contained isolated strips of $(4 \times 4)_1$ blocks, intergrown coherently and randomly in unchanged $(5 \times 4)_1$ block structure. Very rarely seen, however, were also places in which the $(5 \times 4)_1$ blocks showed most unusual image contrast, as if undergoing some 'premonitory' distortion before the actual loss of a row of octahedral groups (Fig. 3a). We return later to the possible significance of this observation, when discussing the reaction mechanism. In Fig. 3a,

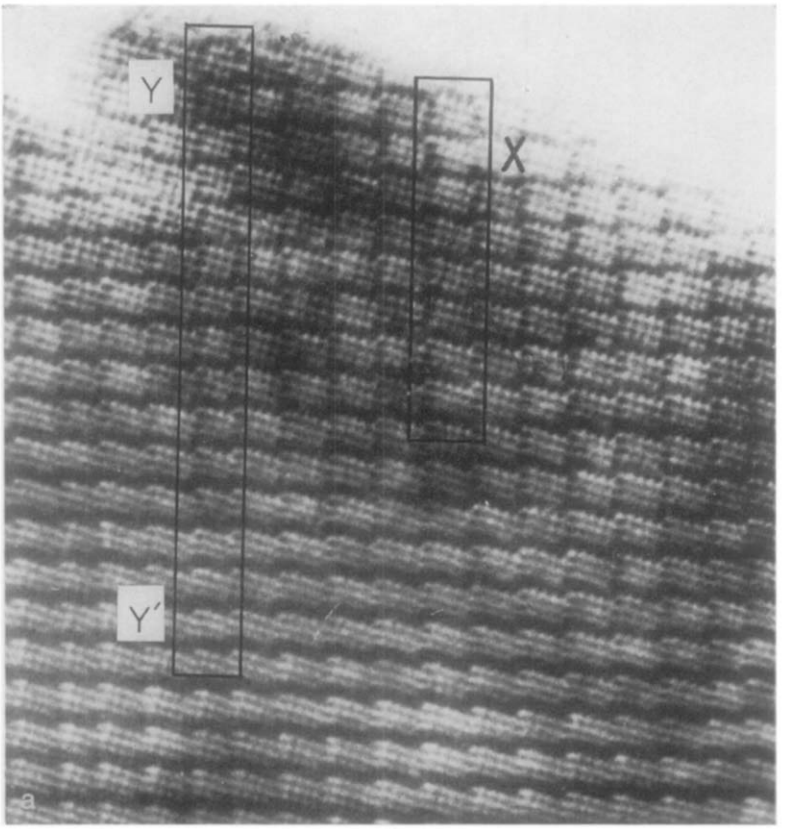

FIG. 3. (a) $8Nb_2O_5.5WO_3$ heated 23 hr at 900°C. For enclosed areas *X*, *Y* see text.

TABLE II

DISPROPORTIONATION $8Nb_2O_5.5WO_3 \rightarrow 7Nb_2O_5.3WO_3 + Nb_2O_5.WO_3$ AT 900°C

Duration of heating	Structure of products
23 hr	Unchanged $(5 \times 4)_1$ block structure with rare intergrowth of $(4 \times 4)_1$ blocks. Some signs of "premonitory" rearrangement.
112 hr	Extensive conversion of $(5 \times 4)_1$ blocks to $(4 \times 4)_1$ blocks. Domains of anomalous structure enriched in WO_3.
495 hr	Conversion still incomplete. Domains of residual $(5 \times 4)_1$ blocks. Intergrown strips of (metastable) $(5 \times 5)_1$ structure.

the appearance of the individual (5×4) blocks is everywhere normal; each has three rows of four white contrast dots, indicative of the 0.28 nm square channels through the ReO_3 structure, except at such places as *X* and *Y*. At *X*, a (4×4) square within a (5×4) block is distinctly differentiated from the remaining row of octahedra, and the "split" continues into the blocks above, along a line parallel to one of the ReO_3 subcell axes. At *Y*, there are lines of (4×4) blocks which are, however, distinctly elongated and, at *Y'*, seem to merge, without any abrupt termination, into a line of (5×4) blocks; all have unusual contrast at their lateral edges.

After 112 hours, reaction was extensive but by no means complete. Some crystal fragments showed little conversion, whereas

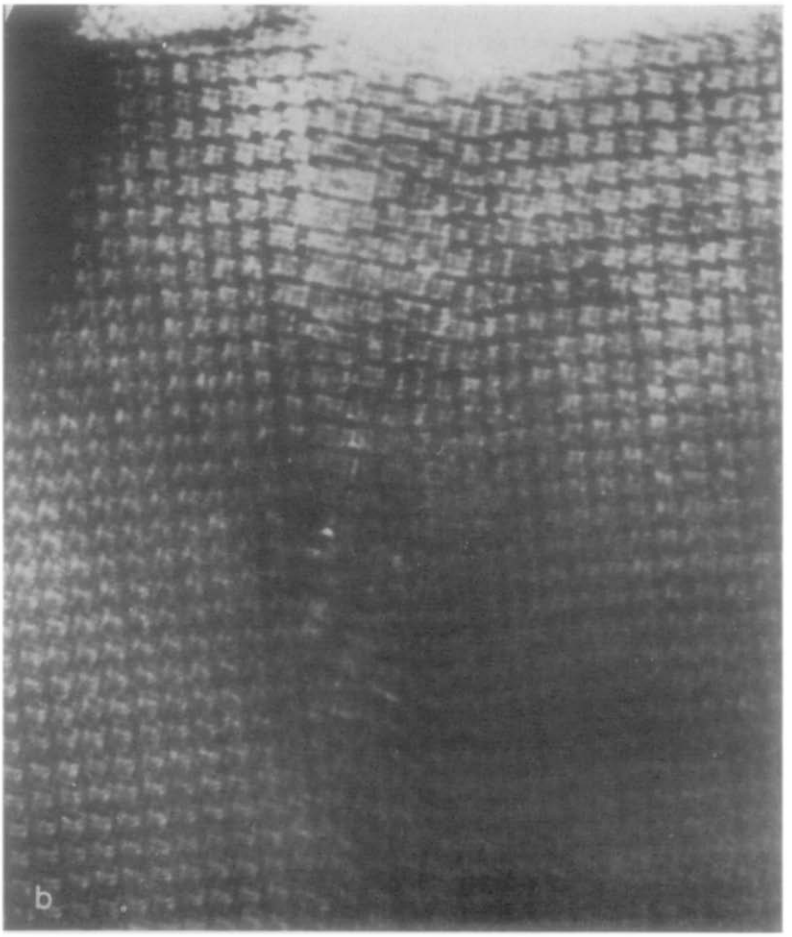

FIG. 3. (b) Domain of anomalous structure in $8Nb_2O_5.5WO_3$ after 112 hours at 900°C.

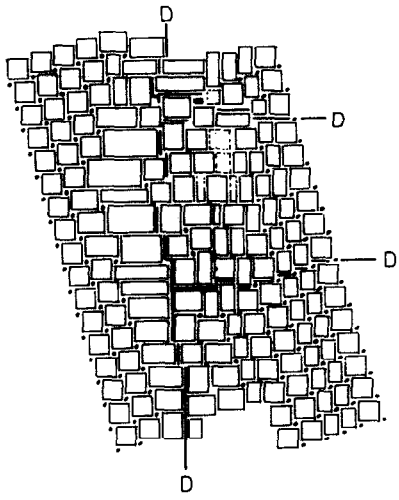

FIG. 4. Structure of the domain shown in Fig. 3. *D* Shows dislocations with partial edge character.

others had extensive domains of $(4 \times 4)_1$ structure in which, however, isolated strips of $(5 \times 4)_1$ parent blocks remained (Fig. 3b). In addition there were occasional faulted areas that may be highly significant. Figure 4 shows the structure of such an area, to be seen in Fig. 3b. It is an irregularly shaped jigsaw of blocks of varied and, in some cases, most unusual dimensions, with cross sections measuring up to (9×5) octahedra. From the relation between cross section and composition of blocks, it can be inferred that such a block has the composition $14Nb_2O_5.17WO_3$; i.e., it is actually richer in WO_3 than the stable product of disproportionation, $Nb_2O_5.WO_3$, which has the topologically different pentagonal tunnel structure. A block-by-block analysis of this domain shows that a set of anomalous, tungsten-rich blocks is interspersed with others that are intermediate in composition between the starting material and the equilibrium product, forming a central region that, in toto, is close to the initial $8Nb_2O_3.5WO_3$, but with a strongly enriched core. This central region abuts, at the right-hand side, on an area that is strongly depleted

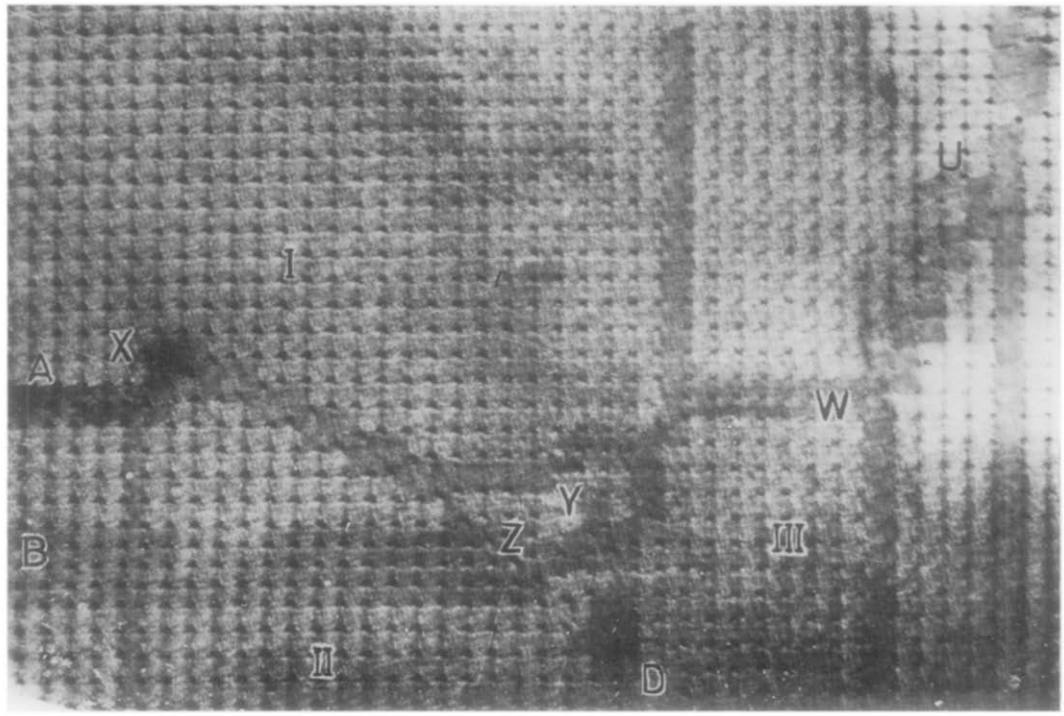

FIG. 5. $9Nb_2O_5.8WO_3$ heated 25 hrs at 1145°C. I, II, III—areas of unchanged structure mutually out of register. A, B, C, D rows of product blocks. U, W rows of WO_3-enriched $(6 \times 5)_1$ blocks. XY—meandering fault originating at dislocation core X.

in WO_3. Thus the whole represents a strong internal fluctuation of composition, in which block interfaces have been extensively readjusted; it also involves several dislocations with partial edge character (*7*). This particular faulted region extended in a meandering line across the thicker part of the crystal flake, where the image cannot be reliably mapped because of dynamical effects, and it terminated in a second domain of anomalous block sizes and compositions. Whilst it is not altogether impossible that the meandering fault could have been present and intrinsic to the original crystal, no such anomalous domains were found either in the original material or in reaction specimens after 23 or 45 hours of heating. Moreover, the domain can be correlated with observations on the reaction of the 9:8 compound. We therefore take both the anomalous fluctuation and the extended fault to be products of the reaction process, and consider later the implications of spontaneous fluctuations of composition.

After very prolonged annealing (495 hours), the material was largely $7Nb_2O_5.3WO_3$, but with intergrown strips of residual $(5 \times 4)_1$ blocks. In addition, there were isolated lines or wider strips of $(5 \times 5)_1$ blocks—i.e., of $9Nb_2O_5.8WO_3$. According to Roth and Waring, the reaction temperature was well below the lower stability limit of that phase. Thus it would appear that a metastable, WO_3-enriched structure is indeed produced, and persists, but has in the progress of time been converted to a highly ordered intergrowth. The evidence suggests that formation of a coherent, but metastable, structure may be more favorable kinetically than some step or steps in the reconstructive process needed to attain equilibrium.

Disproportionation of $9Nb_2O_5.8WO_3$

The low temperature reactions 4 and 5 (Table I) have not yet been studied; the particular interest of the latter was referred to above. Reaction 3 has been examined at 1145–1150°C and reaction 2 at 1200–1230°C. Both give the $(5 \times 4)_1$ structure of the 8:5

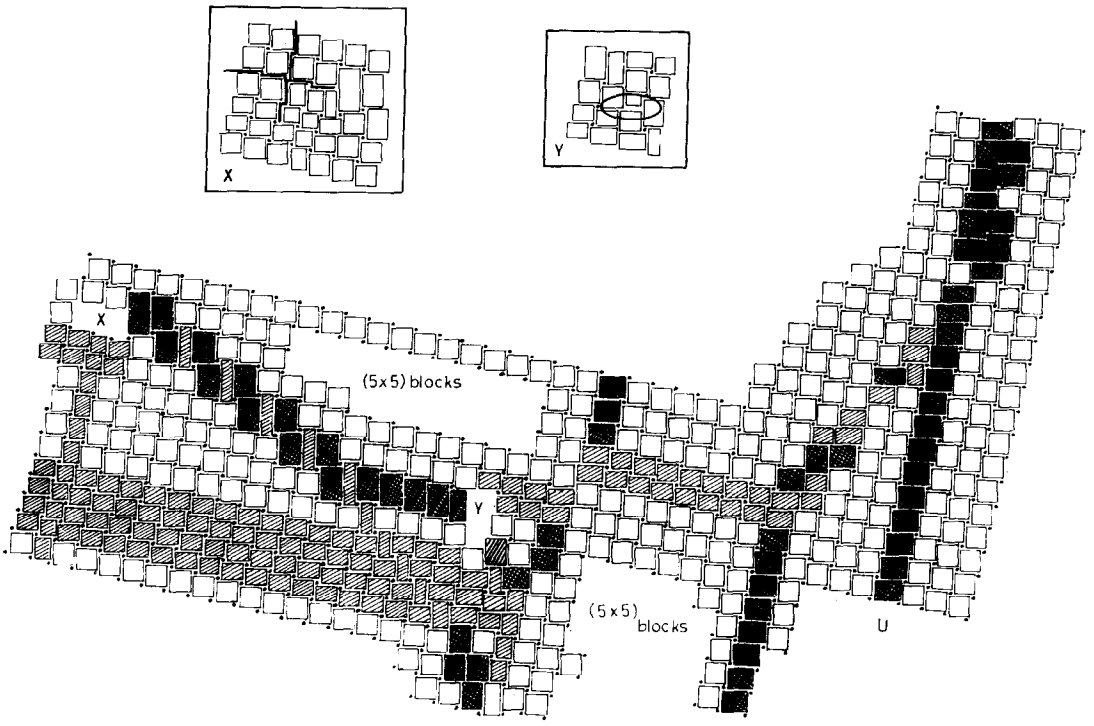

FIG. 6. Structure of area shown in Fig. 5. Lightly hatched blocks: stable product and other blocks depleted in WO_3. Cross hatched blocks: enriched in WO_3.

phase as one product; the other product is likely to differ only in respect of the ordering pattern adopted by filled pentagonal tunnels. Insofar as the homogeneous part of the reaction is concerned, the reactions can be considered together, and any differences can be ascribed chiefly to the greater facility of diffusion and ordering processes at the higher temperature of reaction. The 1145–1150° experiments afford evidence that internal fluctuations and reshuffling processes play a part in the reaction, as in the disproportionation of the 8:5 compound, but (as a result of the higher reaction temperature) to a lesser degree.

After 25 hours at 1145°, the degree of reaction was quite small; the crystals had isolated rows and narrow bands of coherently intergrown product blocks, sparsely distributed. In addition, there were occasional strips or domains of faulted structure, including blocks highly enriched in WO_3.

One such region, which has been fully analyzed, is shown in Fig. 5; its structure is mapped in Fig. 6. The location of tetrahedral sites at the block corners is clearly displayed in Fig. 5, showing that the bulk of the crystal remains as unchanged $(5 \times 5)_1$ structure but that, in the field shown, there are three areas (I, II, III) of this perfect structure which are not in mutual register. On the left-hand side, the lines of tetrahedral sites in the upper and the lower portions are displaced across a meandering fault of abnormal structure; this structure is closely similar to that of other extended defects observed in the partially reacted materials, including that mentioned above in the disproportionation of the 8:5 compound. It is likely that all these faults originate in the internal readjustments of block boundaries that accompany the reactions. Two rows of transformed $(5 \times 4)_1$ blocks, at *A*, and a band of four rows of $(5 \times 4)_1$ blocks, at *B*, run into this fault. At right angles to these, and terminating in the fault, are two isolated rows of $(5 \times 4)_1$ blocks, at *C* and *D*. These product blocks, and all blocks depleted in WO_3, are lightly hatched in Fig. 6. The fault itself originates near the point marked *X* (Fig. 6), and an analysis of the structure around this (7) shows that two dislocations intersect there (Fig. 6, inset). The resulting distortion and warping of lattice planes gives rise to a clearly visible abnormality in image contrast. Two horizontal rows and one vertical row of $(5 \times 4)_1$ blocks terminate in this dislocation; one complete row of oxygen sites has been removed from the crystal to the left of the dislocation, and an additional row of cation sites (i.e., a sheet with the composition MO_2) has been introduced below it. Between *X* and *Z*, the extended fault consists of a succession of similar groups of blocks of unusual dimensions. Each such group of three blocks has the total composition $33Nb_2O_5 . 34WO_3$ and is thus highly enriched in tungsten—again richer in WO_3 than the next stable phase, $Nb_2O_5 . WO_3$. The enriched strip continues, as a row of $(7 \times 5)_1$ blocks ($11Nb_2O_5 . 14WO_3$) to another probable dislocation at *Y*, at which the line of product blocks *D* also terminates. At *Z*, the fault enters the band of product blocks, and changes direction, in the form of another succession of similar units. Each of these (composition $24Nb_2O_5 . 13WO_3$) is somewhat depleted of WO_3, as compared with the adjacent, product $8Nb_2O_5 . 5WO_3$ structure. The micrograph is not well enough resolved to interpret the structure at *Y* unambiguously; the thickness of the crystal, at that point, is in the range where dynamical effects severely hinder delineation of the blocks. However, a mapping based upon the positions of tetrahedral sites and shared block corners (i.e. shared as in $Ti_2Nb_{10}O_{29}$) leaves little doubt that *Y* is a second centre of dislocation, with either a dilated core (as shown inset) or with two edge dislocations emerging from it.

Of the six rows of product blocks that enter the field of the micrograph at A, B, only two are propagated to the right of the center Y. At W they intersect an extended row of enlarged $(6 \times 5)_1$ blocks, with the composition $10Nb_2O_5 . 11WO_3$. This strip is thus again enriched beyond the composition of the next equilibrium phase. The rows of product blocks finally terminate within the crystal, where they meet another row of $(6 \times 5)_1$ blocks U, in a substantially rearranged domain that merits separate consideration. This domain, which joins on to, and somewhat overlaps, the area

shown in Figs. 5 and 6, is shown in Fig. 7 and mapped in Fig. 8. The noteworthy feature is that it consists of a grouping of very unusual blocks—including large $(6 \times 6)_1$ blocks ($11Nb_2O_5.15WO_3$) $(8 \times 4)_1$ blocks ($11Nb_2O_5.11WO_3$) and $(7 \times 5)_1$ blocks ($11Nb_2O_5.14WO_3$)—making a strip just two blocks wide between domains of unchanged $(5 \times 5)_1$ structure. As a result of this interpolated strip, the two unchanged domains are thrown out of register. Within the strip of modified structure, the WO_3-enriched blocks are bordered by blocks that are somewhat depleted in WO_3. Summing up the total composition of the area shown, down to the point where the strip of $(6 \times 5)_1$ blocks *U* terminates, it is found to include $443Nb_2O_5 + 372WO_3$; i.e., the ratio $Nb_2O_5:WO_3 = 1.190$, as compared with $Nb_2O_5:WO_3 = 1.125$ for the parent material. It is a fluctuation that represents a small nett *loss* of WO_3 from that region of crystal, but within it are smaller scale fluctuations, spaced roughly 6 nm apart, within which WO_3 is very markedly *segregated.* Across this strip, two areas of unchanged structure are mutually displaced by $2a_R[110]$ (the suffix denotes the ReO_3 sublattice) and it is reasonable to infer that this is the consequence of an influx of material by diffusion, with such minimal rearrangement of block interfaces as is needed to satisfy the topological requirements of the block structure principle. Figure 8b shows that the notional "original" framework of (5×5) blocks is indeed minimally disturbed by building in the diffusional influx. About 112 additional Nb cations and 26 W cations have been embodied in the strip shown, in each (001) plane of the original tetragonal structure. It may be noted that, within this modified strip, the blocks have assumed a configuration giving long interfaces

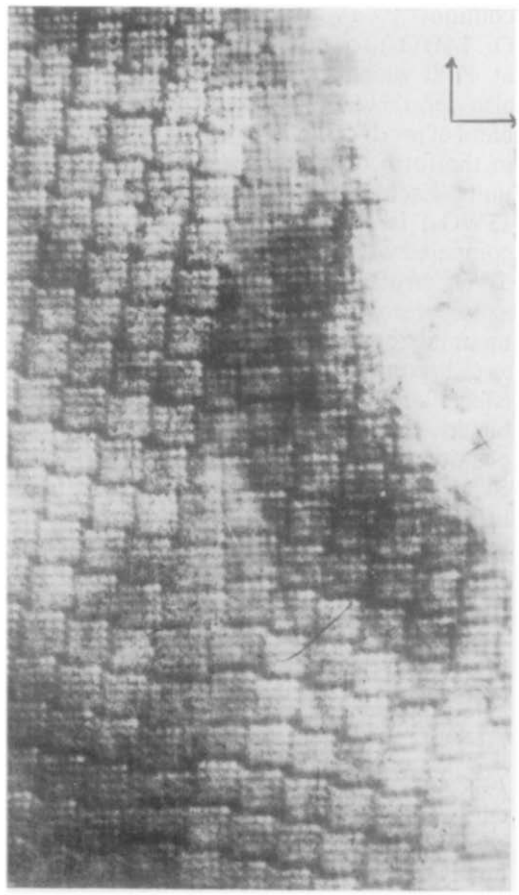

FIG. 7. $9Nb_2O_5.8WO_3$ heated 25 hrs at 1145°C. Strip of abnormal structure inserted in unchanged materials, replacing two rows of $(5 \times 5)_1$ blocks and widening the structure by two rows of octahedra.

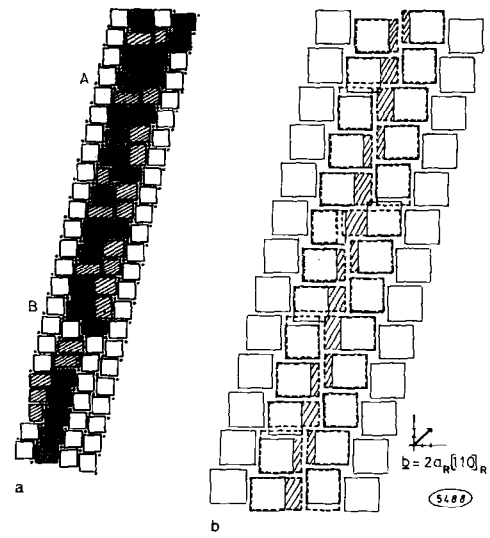

FIG. 8. (a) Structure of the anomalous strip shown in Fig. 7. Hatching of blocks as in Fig. 6. (b) Relation between $(5 \times 5)_1$ blocks in the starting material and the structure of the fault shown in Fig. 8. Unperturbed parts of the crystal are mutually displaced by $2a_R$ 110_R through the insertion of two rows of octahedra (hatched).

parallel to $(100)_R$ and $(010)_R$. The possible significance of this is considered later.

After more prolonged heating at 1145° (72 to 96 hr) the extent of conversion was considerably higher, but still very incomplete. Rows or groups or grouped rows of transformed $(5 \times 4)_1$ blocks were interspersed with isolated rows, broader strips or domains of the unchanged (5×5) structure. Figure 9 shows the structure of a region mapped from one crystal after 72 hours reaction. The lightly hatched rows are those of the reaction product. In the tetragonal $9Nb_2O_5.8WO_3$ structure, a row of octahedra can be equally well removed from the square $(5 \times 5)_1$ blocks along either $(100)_R$ or $(010)_R$, so that the lines of reaction can be introduced in two orthogonal directions. Where such converted strips intersect they necessarily create $(4 \times 4)_1$ blocks (of the $7Nb_2O_5.3WO_3$ structure); their intersection is deficient in tungsten. Shown cross-hatched are two adjacent rows of (5×5) blocks from which one line of tetrahedral sites has been eliminated. Extended faults of this type have been repeatedly found in the 9:8 disproportionation products. The strip has a composition ($19Nb_2O_5.13WO_3$, ratio $Nb_2O_5:WO_3 = 1.45$) intermediate between the initial and final states. However, this change of composition from the matrix material is not simply the elimination of tungsten from tetrahedral sites; each pair of (5×5) blocks must have *lost* 3 tungsten atoms and *acquired* 2 niobium atoms to attain the composition of the structure shown. Such a defect strip is thus a region enriched in niobium. Through the elimination of tetrahedral sites and readjustment of block interfaces, the two domains on either side of the fault strip are mutually displaced by $a_R[100]_R$, corresponding to the elimination of one complete row of octahedra from the structure on one side of the fault. This would imply that some row of product blocks terminates at some point

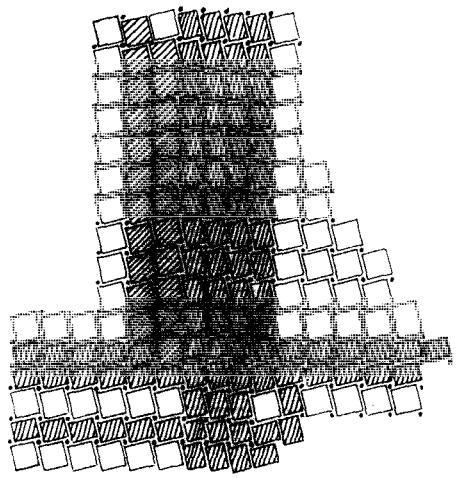

FIG. 9. Structure map taken from micrograph of $9Nb_2O_5.8WO_3$ heated 72 hr at 1145°C, showing intersection of lines of reaction along the equivalent tetragonal axes of the reactant, and elimination of tetrahedral sites between (5×5) blocks to form a strip enriched in Nb_2O_5.

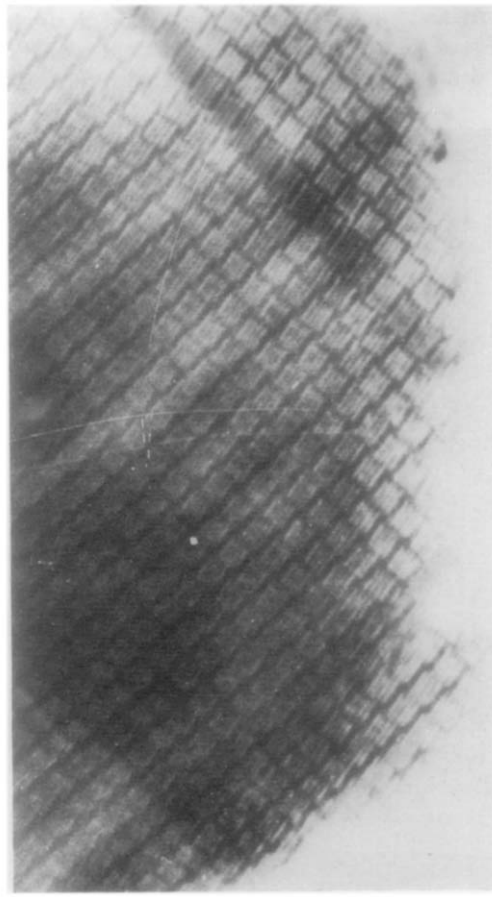

FIG. 10. $9Nb_2O_5.8WO_3$ heated 1 hr at 1230°C. Lines of stable product $(5 \times 4)_1$ blocks and of metastable WO_3-rich $(6 \times 5)_1$ blocks intergrowing, in mutually perpendicular directions.

within the crystal, outside the field of the micrograph.

The characteristics of material reacted at 1200–1230° (reaction 2) were essentially similar. The higher diffusion rates undoubtedly accelerate ordering processes, and we observed no domains of highly abnormal structure, with strong local fluctuations of composition. Coherently intergrown strips of the metastable $(6 \times 5)_1$ block structure ($10Nb_2O_5.11WO_3$) were frequently observed, however, showing that a metastable, WO_3-rich product was formed, but accommodated within a well-ordered structure. It could be observed at an early stage of the reaction. Thus Fig. 10 shows part of a micrograph of material heated one hour at 1230°, with two rows of transformed $(5 \times 4)_1$ structure at *A* and a single row of $(6 \times 5)_1$ blocks at *B*. It is noteworthy, and may be significant for the mechanism of reaction, that rows of tungsten-rich blocks are almost invariably inserted perpendicular, not parallel, to those of the stable product. After 24 hours, transformation was much further advanced, but still very incomplete. Rows of product blocks tended to be present in packets or narrow domains as shown in Figs. 11 and 12. The structure of the region in Fig. 11 is mapped in Fig. 13. In Fig. 11, the lines of product blocks intersect a meandering fault, with a structure very similar to that described previously (Fig. 5), to the right of which, in Fig. 11 they appear to be less compactly grouped. One of the rows of $(5 \times 4)_1$ blocks from the left-hand side of the field shown terminates in this fault, and is associated with a dislocation in the neighbourhood of *D*; one complete row of cation sites is eliminated from the structure below this dislocation. In Fig. 12, the lines of transformed

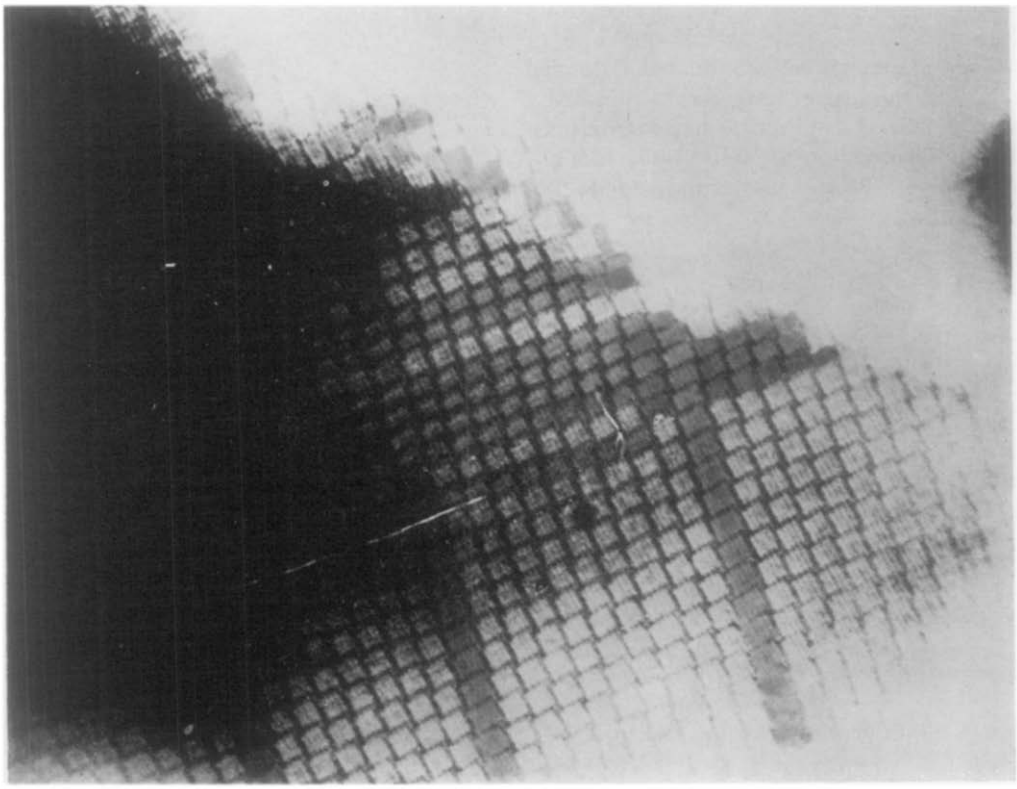

FIG. 11. $9Nb_2O_5.8WO_3$ after 24 hr at 1200°C. Isolated and grouped rows of product blocks, with rows of metastable $(6 \times 5)_1$ blocks, intersecting a meandering fault (compare Figs. 6 and 13), associated with a dislocation at *D*.

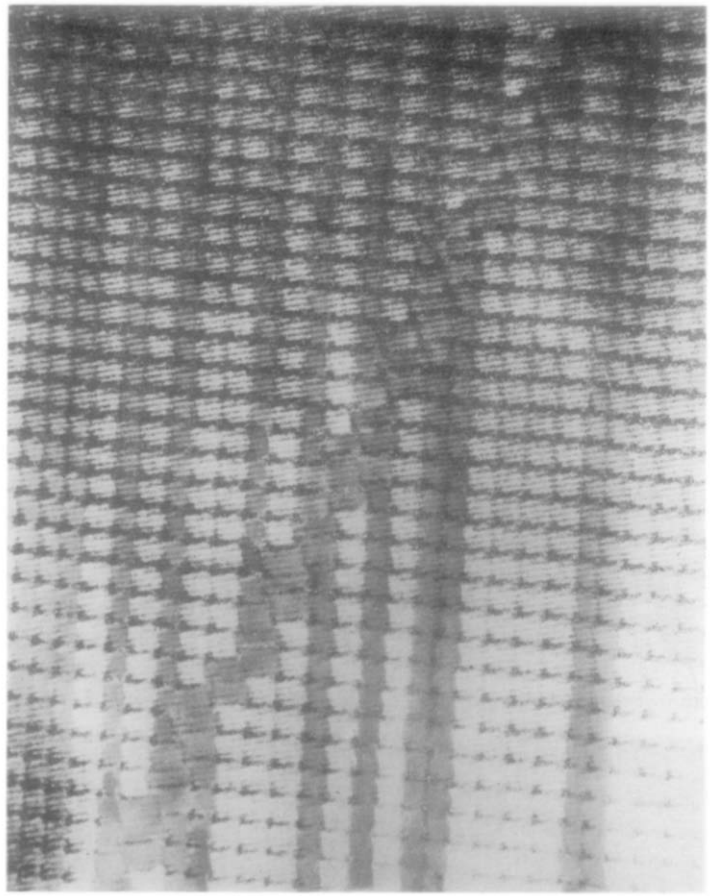

FIG. 12. Meandering fault, across which lines of reacted structure are displaced, in $9Nb_2O_5.8WO_3$ heated 24 hr at 1200°C.

blocks, all running in the same direction, and intersected in the field shown by only one row of metastable, enlarged blocks, also cross a meandering fault of the same type, which was found, in this case, to run right across the crystal flake examined. The repeated occurrence of faults of this type suggests that they arise as a result of the rearrangement of block boundaries within the crystal, and as a frequent accompaniment of reaction. Through these faults, the lines of tetrahedral sites, which serve as position markers for the original structure, are mutually displaced. This displacement indicates either that large sections of crystal structure have been displaced by large-scale cooperative processes, as is discussed below, or else that they are left as residual boundaries between domains within which transformation had proceeded independently.

When reaction is propagated along both the possible orientations, the intersection of the transformed rows of blocks within the crystal necessarily creates a faulted region such as that shown in Fig. 14. In the field shown, six lines of transformed blocks enter from above and five from below; thus one vertical line of (5×4) blocks terminates at the fault. In the other direction, there are two transformed rows on each side, of the intersection, but at *A*, on the left-hand side, there is a row of $(6 \times 5)_1$ blocks which does not cross the fault. The total result of the intersection is that, in the upper right-hand portion of the

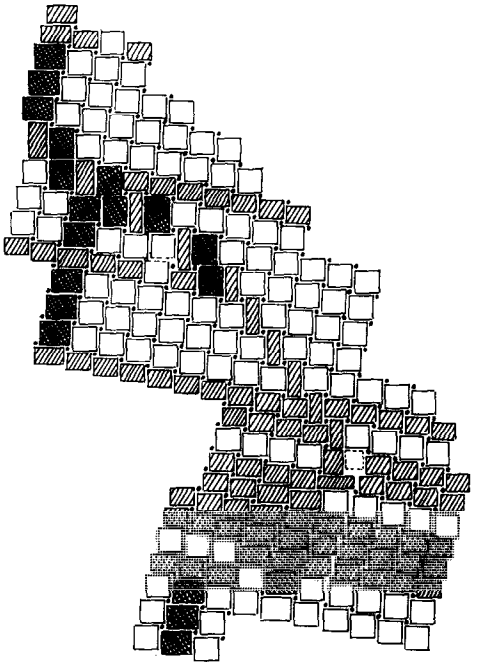

FIG. 13. Structure of region shown in Fig. 11.

field, one complete line of octahedra has been eliminated, both in the vertical and the horizontal directions, so that this portion of crystal is effectively displaced by $a_R(110)_R$ relative to the left-hand and lower portion of the field.

Transformation was nearly complete after 70 hours at 1230° but there remained isolated rows or finite groups of untransformed (5 × 5) blocks. To accommodate finite islands of the (5 × 5) structure coherently, they were necessarily surrounded by faulted, somewhat disordered regions. Thus some inhomogeneities of structure and composition remained; prolonged annealing to eliminate these completely would depend upon the occurrence of large scale cooperative processes and readjustments of block boundaries.

Discussion

The experimental results set out above represent a coroner's inquest into the structures generated during reaction, in which evidence is presented at two levels of reli-

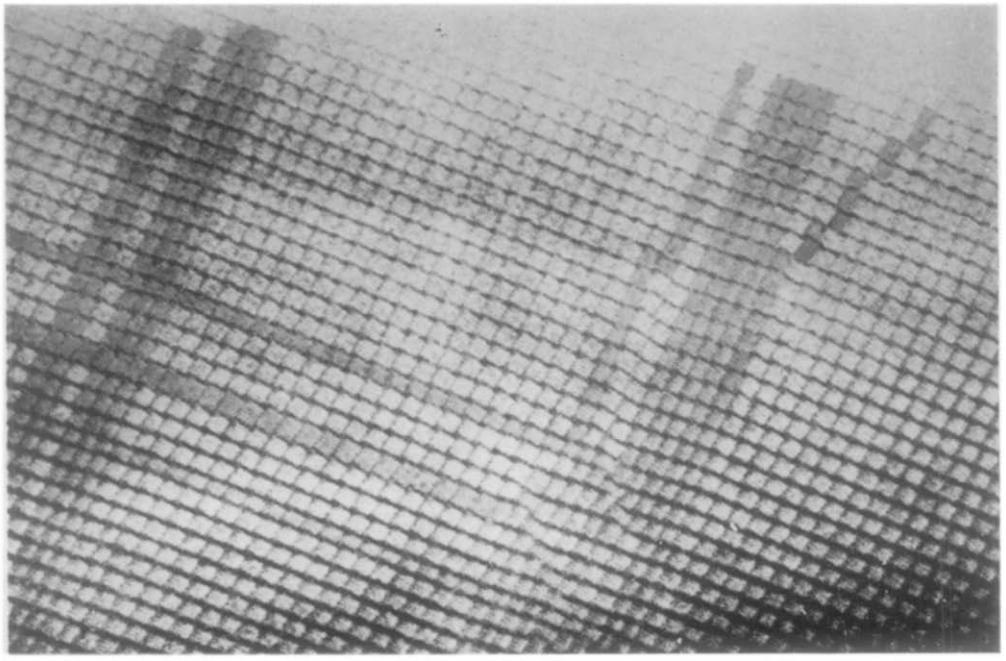

FIG. 14. $9Nb_2O_5.8WO_3$ heated 24 hr at 1200°C. Intersection of rows of product blocks. At *A*, one product row is formed by disproportionation; one vertical and one horizontal row of product effectively terminate in the intersection, generating a displacement of the unchanged parts of the structure. At *D*, evidence suggesting that Wadsley-Andersson migration of *CS* planes enables lines of product to associate into domains.

ability. Most important are those features that are quite general: open to possible question are conclusions drawn from specific and apparently transient structures, where inferences depend upon the hypothesis that these structures are significant for the mechanism of reaction.

As far as block structure reactants and block structure products are concerned, the disproportionations of the 8:5 and the 9:8 compounds are processes of exactly the same type. In both cases, the nett effect is to convert the original structure into one having blocks with their cross sections reduced by one complete row of octahedra. It follows automatically from this that parent and product can intergrow coherently and freely. The evidence given above shows that the process consistently so operates as to convert one line of blocks at a time, block for block, into the reaction product. Unless intersected, displaced or cancelled by some stoichiometric fluctuation, fault or internal boundary, the line of converted structure in due course runs right across the crystal. Lines of product blocks may, in some cases, perhaps have terminated at preexisting faults but, having regard to the perfection of the original material, it is likely that faulted or rearranged structure around the termination of such a line of blocks is itself significant for the way in which reaction is propagated. As has been seen, the lines of product blocks are frequently isolated, or are grouped in small packets, and they show no systematic ordering. These observations strongly suggest that each such line of blocks is the result of a separately initiated, linearly propagated process. The reaction does not proceed by loss of WO_3 from a surface layer, followed by an inward-moving, cooperative readjustment of *CS*-plane boundaries, according to the Wadsley–Andersson concept (*8*).

It may be noted that this linear propagation, in which one sheet of structure at a time is stripped out of the crystal, bears a strong formal resemblance to the way in which *CS* planes are introduced during the reduction of TiO_2 or WO_3. While the mechanism of that process is not yet fully understood, it seems likely that it proceeds by the climb of a dislocation through the crystal, from some nucleating collapsed vacancy disc or interstitial disc, whereby a whole sheet of sites is eliminated from the structure (*9*). The neighborhood of the bounding dislocation line is the main locus of continuing reaction, In the present case, a double sheet of sites must be eliminated: one sheet of anion sites only, the other sheet containing both anion sites and cation sites, with the composition MO_2. The total collapse vector for such a process, $a_R[100]_R$, is a perfect vector of both the anion and the cation sublattices, so that its operation would not introduce any mismatch or antiphase relations in the linkage of coordination octahedra as the structure joined up around the dislocation (*7*). We return later to the role of dislocations in the reaction.

Since the reaction appears to involve a block by block conversion, the chemistry of the process should be expressed on that basis, not merely as an abstraction of WO_3:

Disproportionation of the 8:5 compound:

$$(5 \times 4)_1 \text{ block} \rightarrow (4 \times 4)_1 \text{ block}$$

$$8Nb_2O_5.5WO_3 \rightarrow 7N_2O_3.3WO_3 + (Nb_2O_5 + 2WO_3)$$

Disproportionation of the 9:8 compound:

$$(5 \times 5)_1 \text{ block} \rightarrow (5 \times 4)_1 \text{ block}$$

$$9Nb_2O_5.8WO_3 \rightarrow 8Nb_2O_5.5WO_3 + (Nb_2O_5 + 3WO_3)$$

It follows that although the heterogeneous step in the reaction could be represented as requiring only the transfer of WO_3—that is,

$$8Nb_2O_5.5WO_3 + 3WO_3 \rightarrow 8(Nb_2O_5.WO_3)$$

from block structure to some surface reaction site—the real internal processes within the block structure involve the transport of both niobium and tungsten, away from the linearly propagating reaction front to some other locus of reaction. This must ultimately be the surface where the transfer step occurs, but may proximately be some "sink" for excess WO_3. The heterogeneous surface step itself can be written in terms either of WO_3 transfer alone,

as above, or of the transfer of both niobium and tungsten oxides:

$$8Nb_2O_5.5WO_3 + 3(Nb_2O_5 + 2WO_3) \rightarrow 11(Nb_2O_5.WO_3)$$

$$3(9Nb_2O_5.8WO_3) + 49(Nb_2O_5 + 3WO_3) \rightarrow 19(4Nb_2O_5.9WO_3)$$

WO_3 would certainly be available for phase-to-phase transfer, through the gas phase or by surface diffusion, in simple or polymeric molecular form. The complexity of oxide vapor species at high temperatures, as shown, for example, by the mass spectrometric results of Gilles and his co-workers (*10*), makes it not unlikely that mixed niobium–tungsten oxides could play an important role. If WO_3 alone is transferred, Nb_2O_5 must be "dumped" and it is probable that new, niobium-rich block structure should be built up at the surface. There is no direct evidence for or against this.

As regards the mechanism of the reactions, one important point is that propagation does not appear to depend upon establishing a gradient of chemical potential through the crystals, as a result of depletion of WO_3 at the surface. The evidence for this is found in the anomalous domains (e.g. Fig. 3c) and in the formation of ordered intergrowth of metastable, large blocks—$(6 \times 5)_1$ blocks in the transformation of the 9:8 compound, $(5 \times 5)_1$ blocks from the 8:5 compound. The large blocks in the random domains represent material particularly highly, but locally, enriched in WO_3, but such differences as are observed between the 9:8 and 8:5 disproportionations can be ascribed to the different temperatures of reaction. In both cases, the chemical potential of WO_3 must be raised above the equilibrium value set by coexistence of the 8:5 and TTB phases, or the 7:3 and 1:1 phases, respectively. A supersaturation of WO_3 is set up by internal fluctuations of composition, accompanied by the necessary adjustment of structure. This supersaturation provides a driving force for the transport process that controls the supply and transfer step of WO_3 at the surface, and for the nucleation and growth of the incoherent product. Internal processes within the block structure overshoot the equilibrium value. This can be understood in terms of a schematic-free energy diagram (Fig. 15). In Fig. 15a, the randomized domain and its WO_3-rich fluctuations can be approximated to a nonstoichiometric solid solution; in Fig. 15b, the $(6 \times 5)_1$ blocks of $10Nb_2O_5.11WO_3$ represent elements of a virtual, new line phase. In both cases, the total free energy of the system can be lowered by the coexistence of the stable Nb-rich product with a metastable W-rich intermediate, but the chemical potential of WO_3 for this coherent system is higher than would correspond to the heterogeneous coexistence of stable block structure with stable pentagonal tunnel structure. This state of affairs is revealed because the solid state processes are sluggish enough to preserve the pseudo-equilibrium structures, at least in vestigial amounts.

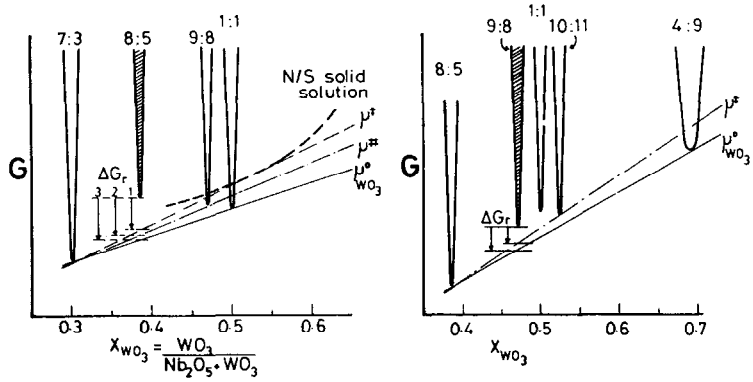

FIG. 15. Schematic free energy diagrams for stabilization of metastable, WO_3-enriched structures: (a) non-stoichiometric domains in $8Nb_2O_5.5WO_3$; (b) $10Nb_2O_5.11WO_3$ in $9Nb_2O_5.8WO_3$.

Three processes must be considered at the mechanistic, microscopic level: lattice diffusion, the role of dislocations and coooperative processes. Unlike the formation of *CS* planes in the reduction of oxides, the linear propagation reaction depends upon simultaneous, short range diffusion processes. The evidence from crystal structures (including unpublished neutron diffraction work by Cheetham and his co-workers at Oxford) is that tungsten and niobium atoms are randomly distributed over the cation sites within the blocks. The reactions however, require that tungsten and niobium should be removed from each block in stoichiometrically appropriate amounts, and this can happen only as place exchange processes permit of some reshuffling of cations within the block. The cations and oxygen atoms that are stripped out of the structure must eventually be transported to and react at the surface. Fluctuations of local composition arising during this process may be preserved by quenching as elements of metastable structure. It cannot be ruled out that lattice diffusion is accelerated by the role of dislocations or some cooperative aspect of the reaction mechanism.

By analogy with the mechanism proposed for the introduction of *CS* planes in the reduction of oxides, it is not unlikely that dislocations should play a part in the linear propagation of the disproportionation reactions. Reaction commencing within some small region of crystal could lead to the formation of a disc of collapse, bounded by a dislocation loop which then climbs through the crystal and itself constitutes the locus of preferred reaction. Such a mechanism is shown schematically in Fig. 16. The ultimate collapse vector, $a_R[100]_R$ could be attained in two ways. Elements of both anion rows and cation rows—i.e., complete coordination octahedra—might be removed in one step, as shown at *A*; alternatively, as at *B*, the large

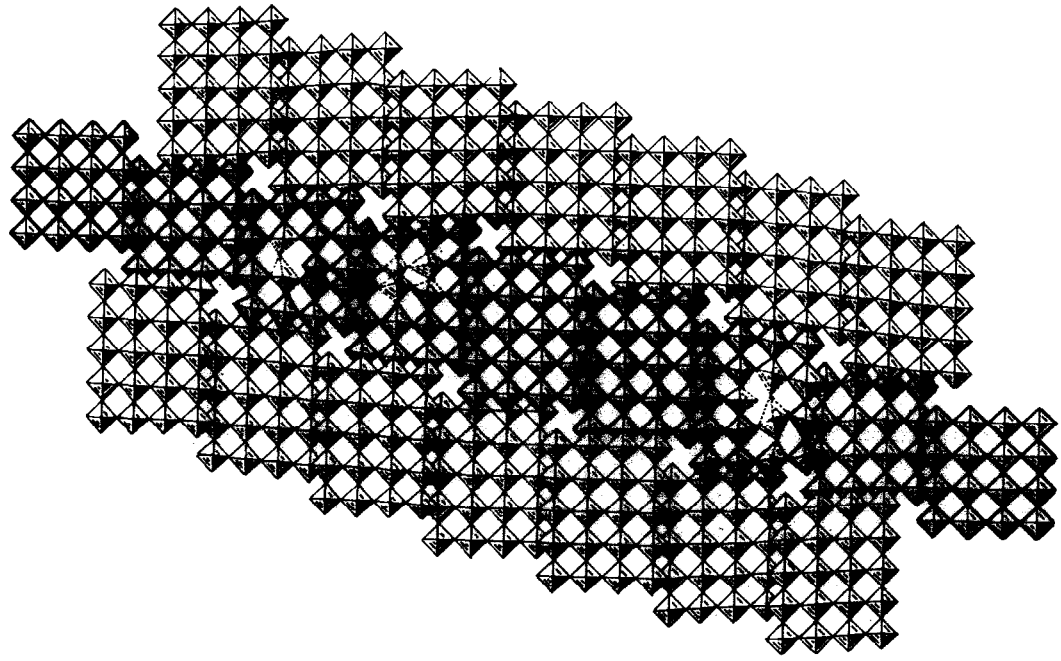

FIG. 16. Schematic representation of dislocation mechanism for stripping out a row of octahedra. (A) by a 1-step process, displacement vector $\mathbf{b} = a_R$; (B) by a 2-step process, with closely spaced partials having $\mathbf{b} = \frac{1}{2}a_R$, removing an anion sheet and a cation (MO_2) sheet successively.

dislocation might split into two partials, with Burgers' vectors $\frac{1}{2}a_R[110]_R$ and $\frac{1}{2}a_R[1\bar{1}0]_R$, whereby first one row of atoms and then the other are removed successively. The one-step process *A* involves a considerably larger dilation and distortion of the adjacent crystal structure.

As has been noted above, dislocations with full or partial edge character have been observed, although not very frequently, in association with lines of reaction terminating within the crystals. However, the operation of a dislocation may not be subsequently identifiable if the strained structure can relax by an appropriate glide, since the total collapse vector is a perfect vector of the structure, which can join up—with its modified chemistry—without dimensional mismatch between blocks.

Direct evidence that dislocations provide the operative mechanism is lacking. When product block rows terminate within a crystal we have occasionally observed an unusual degree of distortion, in that the image contrast shows abnormalities that would be consistent with the dilation of blocks close to the point where rows of atoms have been removed, or where there is compressive strain through the insertion of atom rows (Fig. 3a). Such an interpretation probably leans too heavily upon a simplistic view of lattice image contrast; the observations are recorded, rather than advanced as evidence for a dislocation mechanism.

Reference has been made to the possibility that the change in dimensions, occurring when a row of octahedra is eliminated, could be accommodated by glide. In a number of micrographs (e.g. Figs. 5 and 9) and, indeed, wherever a product row is inserted it can be seen that regions of completely unperturbed structure are bodily displaced and put out of register. This is most obvious where a row of product blocks (whether stable or metastable) terminates within the crystal—i.e., where rows of octahedra have been removed, or where additional octahedron rows have been inserted to create an anomalous domain. In such cases, as shown in Fig. 7, large blocks are formed and so grouped that they present rather extended, continuous interfaces lying along the axes of the DO_9 substructure. This feature is of interest, in that the {100} planes of the DO_9 structure are its most closely packed planes and—although direct evidence is lacking—are likely to be favored glide planes. The block structures are somewhat more complex superstructures of the DO_9 type, in which the local structure and local composition are interrelated; this interplay may lead to some rearrangement of *CS* interfaces which ultimately imposes a jogged configuration on the boundaries between partially transformed and untransformed material. Over long distances, this jogging may generate the type of meandering boundary found repeatedly and illustrated in Figs. 3c and 5. Reaction necessarily brings about a change in over-all dimensions and we suggest that the cooperative process of glide plays an essential part in accommodating it.

A second type of cooperative process is that involved in the Wadsley–Andersson mechanism for migration of *CS*-plane interfaces (*1*, *8*). As stated earlier, it is evident that the reaction as a whole does not proceed from the surface inwards, by this mechanism. However, in the transport of niobium and tungsten through the structure, which may be associated with the formation of the domains of anomalous structure, it may well be that the Wadsley–Andersson process—a switching of linear arrays of octahedral groups from one block to another—plays some part. The nett transport process and the fluctuations of local composition associated with it, may take place along fortuitous but, once established, defined reaction paths, within which this mechanism provides a continuous readjustment of block interfaces. At any instant, these conform to the requirements of the local composition; on quenching, their frozen-in relics are identifiable as the anomalous domains.

It is of interest that the Wadsley–Andersson process seems to operate only for local readjustment of column cross sections. In principle, rows of the stable and metastable products of disproportionation of $9Nb_2O_5 . 8WO_3$ could be produced by a simple Wadsley–Andersson shift: a *CS* interface undergoing a unit displacement along a whole row of

blocks and transferring a row of octahedra (2[NbO_6] and 3[WO_6] groups) from one block to its neighbor.

$$2(5 \times 5)_1 \rightarrow (4 \times 5)_1 + (6 \times 5)_1$$

$$2(9Nb_2O_5.8WO_3) \rightarrow 8Nb_2O_5.5WO_3 + 10Nb_2O_5.11WO_3$$

There is no evidence that this occurs to any significant extent. Its effect would be to create *parallel* rows of $(4 \times 5)_1$ and $(6 \times 5)_1$ blocks, which are not found; instead, as stated, rows of $(6 \times 5)_1$ blocks run *perpendicular* to those of $(4 \times 5)_1$ blocks and this can only result from longer range diffusion transport. In the reaction of $8Nb_2O_5.5WO_3$, the observed, metastable $(5 \times 5)_1$ blocks cannot be produced in an analogous way. The stable product is formed by stripping out a row of four octahedra (2[NbO_6] and 2[WO_6], so that a Wadsley–Andersson *CS* shift would give a different disproportionation product:

$$2(5 \times 4)_1 \rightarrow (4 \times 4)_1 + (6 \times 4)_1$$

$$2(8Nb_2O_5.5WO_3) \rightarrow 7Nb_2O_5.3WO_3 + 9Nb_2O_5.7WO_3$$

A metastable product $9Nb_2O_5.8WO_3$ with $(5 \times 5)_1$ blocks could be formed only if diffusion-transported WO_3 were incorporated simultaneously:

$$2(8Nb_2O_5.5WO_3) + WO_3 \rightarrow 7Nb_2O_5.3WO_3 + 9Nb_2O_5.8WO_3$$

Again, the products would be formed in parallel rows, contrary to the observations. However, rows of $(6 \times 4)_2$ blocks have occasionally been observed, and in the predicted orientation; such a row can be seen in Fig. 12. It may be that a Wadsley–Andersson shift of *CS* interfaces represents one possible route for the reactions, but its role is, at most, a subordinate one.

Acknowledgments

The authors are indebted to the Science Research Council for its support of this work, and to their colleagues, particularly Dr. J. L. Hutchison and Dr. P. L. Gai, for useful discussions. H.O. would thank the Central Research Laboratory, Hitachi Ltd., for leave of absence, during which this work was carried out.

References

1. J. M. Browne and J. S. Anderson, *Proc. Roy. Soc. London, Ser. A* **339**, 463 (1974).
2. R. S. Roth and J. L. Waring, *J. Res. Nat. Bur. Stand.* **70A**, 281 (1966).
3. B. G. Hyde and M. A. O'Keeffe, *Acta Crystallogr.* **A29**, 243 (1973).
4. H. Obayashi and J. S. Anderson, *J. Solid State Chem.* **17**, 79 (1976).
5. R. S. Roth and A. D. Wadsley, *Acta Crystallogr.* **19**, 26, 32 (1965).
6. P. L. Fejes, S. Iijima, and J. M. Cowley. *Acta Crystallogr.* **A29**, 710 (1973).
7. J. S. Anderson, J. L. Hutchison and F. J. Lincoln, *Proc. Roy. Soc. London, Ser. A*, in press.
8. A. D. Wadsley and S. Andersson, *Nature* **211**, 581 (1966).
9. B. G. Hyde and J. S. Anderson, *J. Phys. Chem. Solids* **28**, 1393 (1967).
10. S. L. Bennett, S.-S. Lin, and P. W. Gilles, *J. Phys. Chem.* **78**, 266 (1974).